### Title

Preference of Arabidopsis thaliana GH3.5 acyl amido synthetase for growth versus defense hormone acyl substrates is dictated by concentration of amino acid substrate aspartate




### Authors

Mackelprang, Rebecca
Okrent, Rachel A
Wildermuth, Mary C



### Publication Date

2017-11-01

### DOI

10.1016/j.phytochem.2017.07.001

Peer reviewed

Phytochemistry 143 (2017) 19–28

Contents lists available at ScienceDirect

Phytochemistry

journal homepage: www.elsevier.com/locate/phytochem

# Preference of *Arabidopsis thaliana* GH3.5 acyl amido synthetase for growth versus defense hormone acyl substrates is dictated by concentration of amino acid substrate aspartate

Rebecca Mackelprang, Rachel A. Okrent [1], Mary C. Wildermuth*

*Department of Plant and Microbial Biology, University of California, Berkeley, CA 94720-3102, USA*

ARTICLE INFO

*Article history:*
Received 30 March 2017
Received in revised form
29 June 2017
Accepted 4 July 2017
Available online 23 July 2017

*Chemical compounds studied in this article:*
Salicylic acid (PubChem CID: 338)
Indole-3-acetic acid (PubChem CID: 802)
L-aspartic acid (PubChem CID: 5960)
Indolyl-3-aspartic acid (PubChem CID: 446620)
Salicyloylaspartic acid (PubChem CID: 4520077)
Indole-3-carboxylic acid (PubChem CID: 69867)
Indole-3-butryic acid (PubChem CID: 8617)
Indole-3-pyruvic acid (PubChem CID: 803)
Phenylacetic acid (PubChem CID: 999)
1-Naphthaleneacetic acid (PubChem CID: 6862)
4-Hydroxybenzoic acid (PubChem CID: 135)

*Keywords:*
*Arabidopsis thaliana (Brassicaceae)*
Hormone crosstalk
Hormone homeostasis
Salicylic acid
Indole-3-acetic acid
GH3
Adenyl transferase
Acyl amido synthetase
Aspartate

ABSTRACT

The GH3 family of adenylating enzymes conjugate acyl substrates such as the growth hormone indole-3-acetic acid (IAA) to amino acids via a two-step reaction of acyl substrate adenylation followed by amino acid conjugation. *Arabidopsis thaliana* GH3.5 was previously shown to be unusual in that it could adenylate both IAA and the defense hormone salicylic acid (SA, 2-hydroxybenzoate). Our detailed studies of the kinetics of GH3.5 on a variety of auxin and benzoate substrates provides insight into the acyl preference and reaction mechanism of GH3.5. For example, we found GH3.5 activity on substituted benzoates is not defined by the substitution position as it is for GH3.12/PBS3. Most importantly, we show that GH3.5 strongly prefers Asp as the amino acid conjugate and that the concentration of Asp dictates the functional activity of GH3.5 on IAA vs. SA. Not only is Asp used in amino acid biosynthesis, but it also plays an important role in nitrogen mobilization and in the production of downstream metabolites, including pipecolic acid which propagates defense systemically. During active growth, [IAA] and [Asp] are high and the catalytic efficiency ($k_{cat}/K_m$) of GH3.5 for IAA is 360-fold higher than with SA. *GH3.5* is expressed under these conditions and conversion of IAA to inactive IAA-Asp would provide fine spatial and temporal control over local auxin developmental responses. By contrast, [SA] is dramatically elevated in response to (hemi)-biotrophic pathogens which also induce *GH3.5* expression. Under these conditions, [Asp] is low and GH3.5 has equal affinity ($K_m$) for SA and IAA with similar catalytic efficiencies. However, the concentration of IAA tends to be very low, well below the $K_m$ for IAA. Therefore, GH3.5 catalyzed formation of SA-Asp would occur, fine-tuning localized defensive responses through conversion of active free SA to SA-Asp. Taken together, we show how GH3.5, with dual activity on IAA and SA, can integrate cellular metabolic status via Asp to provide fine control of growth vs. defense outcomes and hormone homeostasis.



## 1. Introduction

Plant hormones regulate development and response to their environment (Jaillais and Chory, 2010; Robert-Seilaniantz et al., 2011a). Indole-3-acetic acid (IAA – an auxin) and salicylic acid (SA) are plant hormones that predominantly promote development and defense, respectively (Dempsey et al., 2011; Spoel and Dong, 2012;

* Corresponding author.
*E-mail address:* mwildermuth@berkeley.edu (M.C. Wildermuth).
[1] Current address: Forage Seed and Cereal Research, USDA ARS, Corvallis, OR 97331, USA.

http://dx.doi.org/10.1016/j.phytochem.2017.07.001
0031-9422/

Vanneste and Friml, 2009; Woodward and Bartel, 2005). Auxin regulates plant developmental processes such as organogenesis through its accumulation in organ primordia where it binds to its receptor, resulting in the degradation of transcriptional repressors of auxin-associated genes and the transcription of a myriad of auxin-associated genes (Kepinski and Leyser, 2005; Vanneste and Friml, 2009). SA synthesis is induced in response to (hemi)biotrophic pathogens such as the powdery mildew fungus *Golovinomyces orontii* (Dewdney et al., 2000; Wildermuth et al., 2001), the bacterium *Pseudomonas syringae* (Rasmussen et al., 1991), and tobacco mosaic virus (Malamy et al., 1990). When sufficient SA accumulates, the master plant immune regulator NPR1 is stable, active, and properly localized, resulting in the transcription of a suite of genes that mediate a robust local defense (Fu et al., 2012; Wu et al., 2012). Even higher levels of SA accumulate when a pathogen induces a hypersensitive response (HR) with programmed cell death (PCD) (Dempsey et al., 2011).

To control amplified downstream effects of hormones, hormone cellular concentrations are tightly regulated both spatially and temporally. For example, high local levels of SA accumulate and cause cell death in tobacco in response to tobacco mosaic virus or a fungal elicitor. Neighboring cells accumulate moderate levels of SA and mount a local defense response, and more distal cells accumulate minimal SA and mount no defense (Dorey et al., 1997; Huang et al., 2006). For auxin, spatial control of concentration and associated downstream impacts is mediated to a large extent by auxin transport and catabolism (Adamowski and Friml, 2015; Mellor et al., 2016). Furthermore, developmental and environmental context and inputs are integrated to coordinate and fine-tune cellular responses. For example, the atypical E2F transcription factor DEL1, which is only expressed in dividing tissue, promotes cell division by inhibiting endoreduplication, SA accumulation and defense (Chandran et al., 2014; Vlieghe et al., 2005).

Given their opposing roles in promoting growth versus defense, IAA and SA have long been known to act antagonistically (Denancé et al., 2013; Robert-Seilaniantz et al., 2011a). Exogenous auxin can suppress SA-dependent defense (Park et al., 2007a; Robert-Seilaniantz et al., 2011a, 2011b), while exogenous SA treatment decreases *Arabidopsis* biomass in an auxin-dependent manner (Canet et al., 2010). However, a sophisticated understanding of the variety of mechanisms by which IAA and SA modify each other's accumulation, activity, and function with cellular resolution remains limited (Denancé et al., 2013; Robert-Seilaniantz et al., 2011a).

One means by which hormone activity is directly regulated is via conjugation to amino acids. For example, IAA conjugation to Asp initiates auxin catabolism (Ostin et al., 1998), while conjugation to Ala stores IAA as an inactive form that is rapidly reactivated through hydrolysis by a dedicated enzyme (Rampey et al., 2004). The only SA-amino acid conjugate found in plants thus far is salicyloyl-aspartate (SA-Asp) (Bourne et al., 1991; Chen et al., 2013; Steffan et al., 1988). Similar to IAA-Asp, SA-Asp is not hydrolyzed back to SA (Chen et al., 2013). Furthermore, SA-Asp was unable to induce robust defense gene expression (Chen et al., 2013), suggesting SA-Asp, like IAA-Asp, is also an inactive form of the hormone dedicated to catabolism. However, an additional possibility is that it functions as a mobile form of SA involved in low level priming of defense (Chen et al., 2013).

Hormone-amino acid conjugation in plants is catalyzed by enzymes belonging to the GH3 (Gretchen Hagen 3) family which are members of the greater firefly luciferase family of adenylating enzymes (Staswick et al., 2005, 2002). GH3 enzymes are divided into three groups based on syntenic analysis and preferred substrates (Okrent and Wildermuth, 2011; Staswick et al., 2002). Generally, GH3s that conjugate JA are classified as Group I; GH3s that conjugate IAA are classified as Group II (Okrent and Wildermuth, 2011; Staswick et al., 2005); and Group III is less well characterized. In *Arabidopsis*, active acyl substrates are known only for one classic Group III member, GH3.12/PBS3, which prefers 4-substituted benzoates such as 4-hydroxybenzoic acid (4-HBA) and *para*-aminobenzoic acid (pABA) (Okrent et al., 2009; Okrent and Wildermuth, 2011).

Surprisingly, in addition to auxins, the Group II member GH3.5 (At4g27260) is also active on SA and is the only GH3 enzyme known with this activity (Chen et al., 2013; Staswick et al., 2005, 2002; Westfall et al., 2016). Endpoint assays indicated the possibility of GH3.5 conjugation of auxins to a variety of amino acids (Staswick et al., 2005; Wang et al., 2012), though *in planta* measurements point to Asp as the dominant amino acid conjugate (Park et al., 2007a; Zhang et al., 2007). As IAA-Asp and SA-Asp appear to be inactive or hypoactive non-hydrolyzable forms of these hormones, GH3.5 conjugation could play an important role in IAA and SA homeostasis and hormone cross-talk.

To better understand the function of GH3.5 in auxin and SA metabolism and response, we undertook a biochemical kinetic study of GH3.5 to accurately determine its acyl substrate preference for IAA, SA, and related substrates as well as its amino acid substrate preference (e.g. Asp). Kinetic parameters were recently reported for GH3.5 (Westfall et al., 2016). Our contemporaneous, independent examination of the kinetics of GH3.5 on a variety of auxin and benzoate substrates extends these findings. Most notably, we show that GH3.5 strongly prefers Asp as the amino acid conjugate and that the concentration of Asp dictates the functional activity of GH3.5 on IAA vs. SA. High levels of Asp can significantly modify GH3 reaction kinetics with the degree of inhibition dependent on the acyl substrate; therefore, kinetic parameters assessed at one high amino acid concentration may misrepresent GH3 $K_m$'s and acyl substrate preference. Because IAA, SA, and Asp concentrations vary at the cellular level with developmental and environmental context, understanding GH3.5 activity and preference in the context of physiologically-relevant concentrations of these substrates allows us to specifically predict GH3.5 function in a context-dependent manner. These predictions are consistent with observed *GH3.5* gene expression and provide a mechanistic understanding for the dual function of GH3.5 in hormone homeostasis in growth and defense.

## 2. Results and discussion

### 2.1. Kinetic parameters of GH3.5 adenylation on auxin-like substrates

Hormone acyl substrate specificity for GH3.5 was initially explored using an endpoint $PP_i$ Exchange Assay, which found GH3.5 to be active on a variety of auxins and SA (Staswick et al., 2005, 2002). To better understand the preference of GH3.5 for auxins, SA, and related compounds, we employed a high throughput kinetic assay of adenylation (Okrent et al., 2009), shown in Fig. 1. Similar to Staswick et al., 2005, we found GH3.5 was active on auxin-like compounds: IAA, indole-3-pyruvic acid (IPA), indole-3-butyric acid (IBA), indole-3-carboxylic acid (ICA), 2-phenylacetic acid (PAA) and the synthetic auxin 1-napthaleneacetic acid (NAA) (Fig. 2). GH3.5 exhibited the greatest affinity for IAA ($K_m = 45$ μM) and least for IBA ($K_m = 733$ μM). The $V_{max}$ of all auxin-like substrates tested were very similar, 53–104 nmol * $min^{-1}$ * $\mu g^{-1}$ (Fig. 2B). The catalytic efficiency ($k_{cat}/K_m$) of GH3.5 was highest with IAA at 5.12 $min^{-1}$ * $mM^{-1}$. Westfall et al. (2016) also found GH3.5 to be active on IAA, PAA, and NAA and to exhibit similar catalytic efficiencies.

As IAA is the dominant auxin, our further studies with GH3.5 focus on IAA as the auxin substrate. However, the ability of GH3.5 to act on a variety of naturally occurring auxin-like substrates is important, as they appear to play distinct roles in both plant

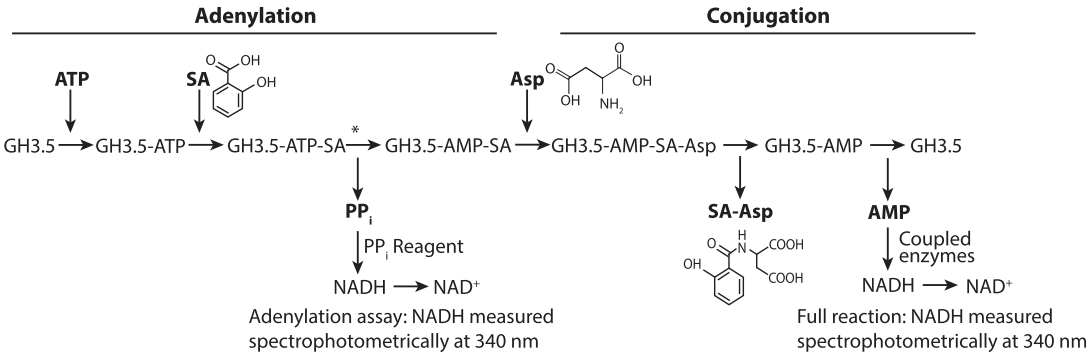


**Fig. 1. Progression of GH3.5 reaction**. GH3.5 enzymatic activity, shown here with SA as the acyl substrate and Asp as the amino acid substrate, appears to proceed via a bi uni uni bi ping pong reaction mechanism: two substrates (ATP and SA) bind to the enzyme, one product ($PP_i$) leaves, another substrate (Asp) binds, and finally two products (SA-Asp and AMP) leave (Chen et al., 2010). The enzyme's C-terminus undergoes a 180° conformation change (*) prior to $PP_i$ release (Westfall et al., 2016). The release of product at two distinct steps allows for measurement of the enzyme activity at two reaction points. Assays were done by either coupling the release of $PP_i$ or AMP to loss of NADH (see methods). Modified from Chen et al. (2010).

development and in plant-microbe interactions (Hagemeier et al., 2001; Schlicht et al., 2013; Sugawara et al., 2015; Tao et al., 2008). In addition, conjugation and inactivation of synthetic auxins such as NAA by GH3.5 or related GH3s could evolve to limit the effect of synthetic auxins as herbicides (which inhibit the function of endogenous auxins). On the other hand, neutralization of synthetic auxin herbicides by engineered or bred plants with herbicide-specific GH3 activity could specifically promote growth of desired plants.

### 2.2. Kinetic parameters of GH3.5 adenylation on benzoate substrates

We found GH3.5 to have a much higher $K_m$ (1171 μM) for SA compared with IAA, with 73-fold lower catalytic efficiency (Fig. 2B). Similarly, Westfall et al. (2016) reported a significantly lower catalytic efficiency with SA compared to IAA. In contrast to GH3.12/PBS3 which is active on multiple 4-subsituted benzoates (4-HBA and 4-ABA/pABA), but not on SA (2-HBA) (Okrent et al., 2009), we found GH3.5 was only active on SA, and not on 2-ABA/anthranilate (Fig. 2). Additionally, GH3.5 was also active on 4-HBA (Fig. 2), showing that GH3.5 substrate preference is not determined by substitution position. GH3.5 exhibited extremely low activity (just above control) with methyl salicylate (MeSA), a transported form of SA (Park et al., 2007b). However, due to its limited activity, we could not reliably calculate kinetic parameters with MeSA.

To gain further insight into GH3.5 acyl substrate preferences, we looked at the binding site using UCSF Chimera (Pettersen et al., 2004) to overlay the crystal structures for GH3.5 with AMP and IAA bound (Westfall et al., 2016) and PBS3 with AMP and SA (an inhibitor of PBS3) bound (Westfall et al., 2012). The PBS3 crystal structure shows the carboxylic acid group of SA is unable to bind to AMP as it is oriented in the opposite direction, bound to Tyr120 and Arg123. In GH3.5, Leu137 replaces Arg123 and our modeling shows Leu137 would be unable to hold SA in the nonproductive orientation. In addition, GH3.5 Met337 may spatially exclude SA from binding to GH3.5 in the inhibitory orientation, as it extends further into the binding pocket than the PBS3 analogue Thr324. Additional GH3 crystal structures coupled with kinetic characterization of wild type and site-directed mutants should further resolve residues that dictate inhibitory and productive acyl substrate binding in the active site.

### 2.3. GH3.5 utilizes Asp as its amino acid substrate

Thin layer chromatography end point assays suggested GH3.5 can conjugate Asp, Glu, and several other amino acids to IAA (Staswick et al., 2005). Using a high throughput kinetic assay for the full reaction (see methods), which is based on real time values of the final product AMP (Fig. 1), we determined that GH3.5 utilizes Asp as its preferred amino acid substrate (Fig. 3). Results with IAA or SA as the acyl substrate showed minimal activity with Glu. GH3.5 was also reported to conjugate ICA to Cys to form an intermediate in the synthesis of the phytoalexin camalexin (Wang et al., 2012). However, we saw no evidence for this activity using our full kinetic assay. Wang et al. (2012) incubated their reaction for 3 h followed by endpoint product detection by UPLC/ESI-QTOF-MS. While debate continues on camalexin biosynthetic pathways (Geu-Flores et al., 2011; Klein et al., 2013; Møldrup et al., 2013; Su et al., 2013, 2011), our kinetic data indicate GH3.5 is not likely to be directly involved.

Using our high throughput kinetic full reaction assay, we next determined the $K_m$ of GH3.5 for Asp with 1 mM IAA or SA. The $K_m$s of GH3.5 for Asp with IAA or SA are not significantly different, 414 μM and 371 μM, respectively (Table 1). For both SA and IAA, the concentration of Asp had to rise to greater than 1 mM for saturation to occur. Furthermore, physiologically-relevant concentrations of Asp (>3 mM) resulted in significant inhibition (~60% of $V_{max}$) of the full reaction with either IAA or SA, with further inhibition observed at higher [Asp]. OsGH3-8 also exhibited inhibition of the full reaction with IAA with Asp above 5 mM (Chen et al., 2009). Therefore, it is important that assessments of GH3 activity do not routinely employ high levels of amino acid substrates (i.e. >= 3 mM) as in Westfall et al., (2016) as this could misrepresent kinetic parameters as well as acyl and amino acid substrate preference.

### 2.4. GH3.5 preference for IAA versus SA depends on Asp concentration

The cellular concentration of IAA, SA, and Asp varies with development and pathogen infection. Therefore, to provide insight on GH3.5 activity and function in a physiological context, we assessed GH3.5 kinetic parameters for the full reactions of IAA and SA at three physiologically relevant concentrations of Asp: 0.2, 1, and 2.5 mM Asp (Table 2A, Fig. 4A and B).

The full reactions with IAA resulted in similar $K_m$s for IAA of ~20 μM independent of [Asp]. $V_{max}$ increases with [Asp], consistent with our reported $K_m$ for Asp of 414 μM (Table 1) and failure to fully saturate at 1 mM Asp. However, with SA, we obtained an unexpected result. The $K_m$ for SA increased dramatically with increasing [Asp], particularly at 2.5 mM Asp and $V_{max}$ did not increase when [Asp] was increased from 1 to 2.5 mM. Functionally, this results in a 50-fold

A

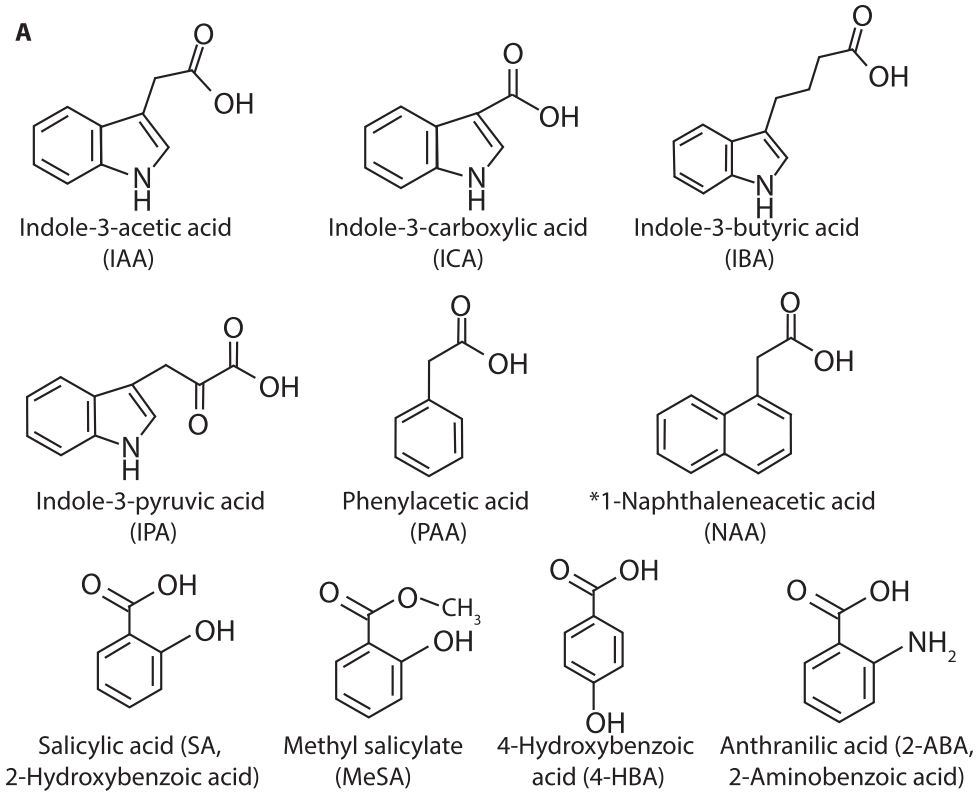


*synthetic auxin

B

| | $K_m$ (μM) | $V_{max}$ (nmol * min$^{-1}$ * μg$^{-1}$) | $k_{cat}$ (min$^{-1}$) | $k_{cat}/K_m$ (min$^{-1}$ * mM$^{-1}$) | katal (mol * s$^{-1}$) |
|---|---|---|---|---|---|
| **IAA** | 45 ± 11 | 66 ± 3 | 0.23 | 5.12 | 0.033 |
| **IBA** | 733 ± 172 | 88 ± 5 | 0.31 | 0.42 | 0.01 |
| **IPA** | 321 ± 94 | 98 ± 9 | 0.34 | 1.06 | 0.009 |
| **ICA** | 501 ± 86 | 96 ± 3 | 0.33 | 0.66 | 0.009 |
| **PAA** | 220 ± 59 | 53 ± 5 | 0.19 | 0.84 | 0.016 |
| **NAA*** | 211 ± 50 | 104 ± 8 | 0.36 | 1.29 | 0.011 |
| | | | | | |
| **SA** | 1171 ± 473 | 24 ± 4 | 0.08 | 0.07 | 0.035 |
| **4-HBA** | 404 ± 80 | 32 ± 2 | 0.11 | 0.27 | 0.027 |
| **MeSA** | -- | -- | -- | -- | -- |
| **2-ABA** | -- | -- | -- | -- | -- |

**Fig. 2. Kinetic parameters of GH3.5 adenylation of auxins and benzoates**. **(A)** Structures of auxins (IAA, ICA, IBA, IPA, PAA, NAA) and benzoates (SA, MeSA, 4-HBA, and 2-ABA) assayed for activity with GH3.5. **(B)** Table showing auxin analogues (top) and benzoates (bottom) that were tested as acyl substrates of GH3.5 in adenylation reactions. Experiments were repeated 3 times, each in triplicate with similar results.

higher affinity for SA at low concentrations of Asp (i.e. 0.2 vs. 2.5 mM Asp). Catalytic efficiency of GH3.5 with SA is also more favorable, with 10-fold higher $k_{cat}/K_m$ at 0.2 and 1 mM Asp than with 2.5 mM Asp. Comparison of GH3.5 preference for IAA vs. SA (Table 2B) shows a dramatic variation with [Asp], with 5-fold higher catalytic efficiency with IAA vs. SA at 0.2 mM Asp and 357-fold higher catalytic efficiency with IAA vs. SA at 2.5 mM Asp.

The $K_m$ for IAA of ~20 μM is in the range of a subset of GH3s that are active on IAA including VvGH3-1, VvOsGH3-8, OsGH3-8, and AtGH3.17 (Böttcher et al., 2012; Chen et al., 2009; Westfall et al., 2016). It is well below that of 770 μM reported for AtGH3.5 by Westfall et al. (2016), assayed with 5 mM Asp. Westfall et al. (2016) also reported high $K_m$'s for IAA for AtGH3.1 and AtGH3.2 (530 and 510 μM), assessed with 10 mM Asn and Asp, respectively. Of the IAA-adenylating GH3 enzymes, only AtGH3.5 is reported to have substantial activity on benzoates with a $K_m$ of 700 μM for SA, assessed at 5 mM Asp (Westfall et al., 2016). At 2.5 mM Asp, our observed AtGH3.5 $K_m$ for SA was similar ($K_m$ = 1.25 mM); however, with decreasing [Asp], the $K_m$

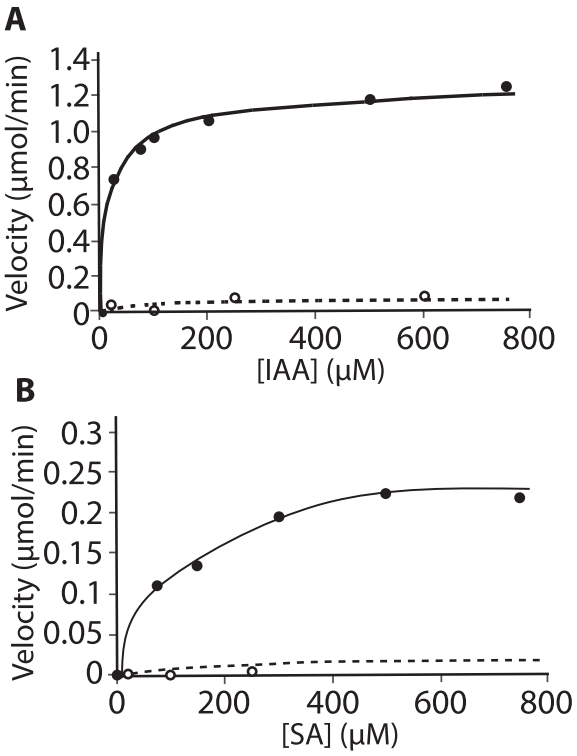


**Fig. 3. Asp is preferred to Glu as the amino acid substrate of GH3.5 with IAA and SA.** Initial velocity measurements of GH3.5 activity show that Asp (●) is preferred to Glu (○) in conjugation reactions with **(A)** IAA and **(B)** SA. Experiments were repeated 3 times, each in triplicate with similar results.

decreased with a $K_m$ for SA of 23 µM at 0.2 mM Asp illustrating the importance of assessing kinetic parameters over a range of physiologically relevant amino acid concentrations.

The double reciprocal plot with IAA and varied Asp shows parallel lines (Fig. 4C), consistent with results obtained for OsGH3-8 and a bi uni uni bi ping pong GH3 reaction mechanism (Chen et al., 2010). For SA, while the 0.2 mM Asp and 1 mM Asp double reciprocal plots have the same slope, the slope at 2.5 mM Asp is much steeper (Fig. 4D) suggestive of competitive inhibition under these conditions.

The crystal structure of GH3.5 (Westfall et al., 2016) is similar to other published GH3 crystal structures (Peat et al., 2012; Westfall et al., 2012). Based on these structures, it appears that the smaller C-terminal domain pivots 180° to move from open (ATP bound) to closed (AMP bound) conformations after the acyl substrate is adenylated (See Fig. 1). $PP_i$ is likely released immediately after the conformation change because $PP_i$ is a competitive inhibitor of Asp and a noncompetitive inhibitor of IAA and ATP (Chen et al., 2010). With the proposed GH3 bi uni uni bi ping pong reaction mechanism, Asp should not affect acyl substrate binding as the acyl substrate and amino acid substrate should bind to different forms of the enzyme (Chen et al., 2010) (Fig. 1). However, Asp and $PP_i$ could act as competitive inhibitors of each other as they are predicted to bind the same form of the enzyme (Chen et al., 2010). We found no significant impact of Asp on SA adenylation measured as $PP_i$ release (not shown), suggesting the SA-dependent impact of Asp at high concentrations may function after $PP_i$ release. Clearly, the reaction profile is altered and deviates from standard Michaelis-Menten kinetics for the GH3.5 reaction with SA at 2.5 mM Asp (Fig. 4B). The crystal structure of GH3.5 does not include Asp, leaving us to speculate about the role of Asp in substrate-specific catalytic efficiency.

## 3. Model for duality of GH3.5 function in hormone homeostasis

Herein, we demonstrate the novel finding that the amino acid concentration can affect the kinetics of a GH3 family enzyme. Mechanistically, this is quite notable. In the previously proposed GH3 bi uni uni bi ping pong reaction mechanism, Asp should not

**Table 1**
Kinetic parameters for Asp with IAA and SA in the full reaction. Independent experiments, run in triplicate, gave similar results.

| | $K_m$ (µM) | $V_{max}$ (nmol * $min^{-1}$ * $\mu g^{-1}$) | $k_{cat}$ ($min^{-1}$) | $k_{cat}/K_m$ ($min^{-1}$ * $mM^{-1}$) | katal (mol * $s^{-1}$) |
|---|---|---|---|---|---|
| IAA | 414 ± 42 | 60.0 ± 2.3 | 0.83 | 2.01 | 0.014 |
| SA | 371 ± 72 | 15.4 ± 1.1 | 0.21 | 0.58 | 0.055 |

**Table 2**
Kinetic Parameters of GH3.5 for IAA and SA in the full reaction with varied [Asp]. **(A)** Comparisons of kinetic parameters of IAA and SA with GH3.5 in the full reaction with varying concentrations of amino acid substrate. Reactions were repeated at least three times, in triplicate. Results showed similar trends, and a representative result is shown. Additionally, similar results were found with independent enzyme preps. **(B)** The catalytic efficiency ($k_{cat}/K_m$) for the full reaction of GH3.5 with IAA compared with SA increases with [Asp].

**A**

| | | Full Reaction | | | | |
|---|---|---|---|---|---|---|
| | | $K_m$ (µM) | $V_{max}$ (nmol * $min^{-1}$ * $\mu g^{-1}$) | $k_{cat}$ ($min^{-1}$) | $k_{cat}/K_m$ ($min^{-1}$ * $mM^{-1}$) | katal (mol * $s^{-1}$) |
| IAA | [Asp] = 0.2 mM | 12 ± 3 | 29.5 ± 1.0 | 0.10 | 8.3 | 0.029 |
| | [Asp] = 1 mM | 22 ± 4 | 120 ± 2.8 | 0.42 | 19.2 | 0.007 |
| | [Asp] = 2.5 mM | 25 ± 1 | 179.4 ± 2.0 | 1.25 | 50.0 | 0.005 |
| SA | [Asp] = 0.2 mM | 23 ± 7 | 2.5 ± 0.1 | 0.04 | 1.6 | 0.336 |
| | [Asp] = 1 mM | 123 ± 23 | 13.6 ± 0.7 | 0.19 | 1.5 | 0.063 |
| | [Asp] = 2.5 mM | 1246 ± 344 | 12.5 ± 1.0 | 0.17 | 0.14 | 0.068 |

**B**

| [Asp] (mM) | Catalytic Efficiency IAA/SA |
|---|---|
| 0.2 | 5 |
| 1 | 13 |
| 2.5 | 357 |

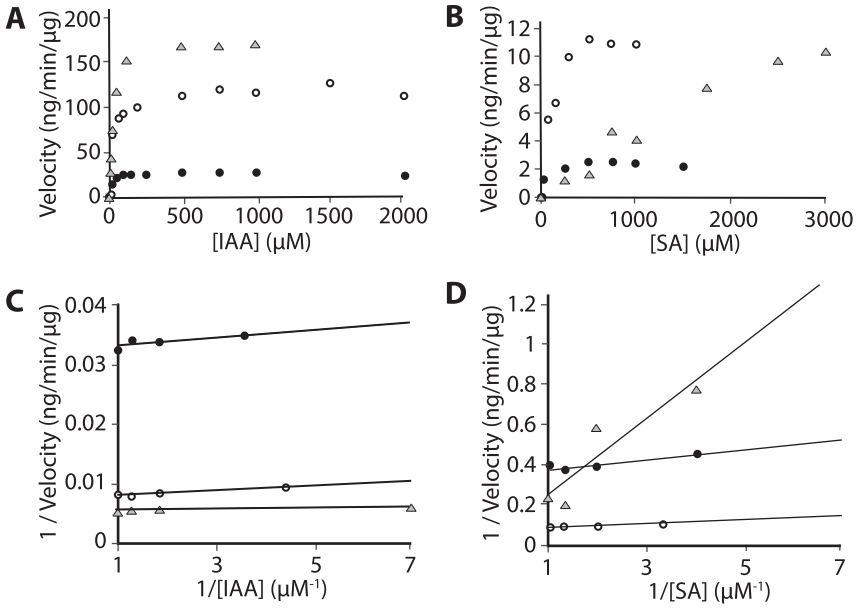


**Fig. 4. Initial velocity and reciprocal plots for IAA and SA full conjugation reactions by GH3.5**. Concentration vs velocity plot for **(A)** IAA and **(B)** SA. While $V_{max}$ is similar in **(B)** for 1 and 2.5 mM, the $K_m$ is much greater with 2.5 mM Asp. Double reciprocal plots for **(C)** IAA and **(D)** SA showing 1/velocity vs 1/concentration acyl substrate, ranging from 0.125 to 1 mM, at fixed ATP (2.5 mM) concentration. Aspartate was varied between 0.2 mM (●), 1 mM (○) and 2.5 mM (△). Parallel lines indicate a lack of competition between Asp and acyl substrate. High concentrations of Asp may lead to Asp competition with SA, but not IAA.

affect binding of the acyl substrate (Chen et al., 2010) (Fig. 1). Indeed, in our work it did not affect IAA. It did, however, affect SA in the full reaction, indicating that, after $PP_i$ is released, Asp can affect the SA-AMP-GH3.5 intermediate, perhaps through alteration of the C-terminus pivot. While several GH3s have been surveyed in recent years, extensive profiling with varied amino acid concentrations has been lacking. We suggest that analysis of one amino acid concentration may be misleading and miss other important information as to enzyme substrate preference.

GH3.5 catalytic efficiency for IAA vs. SA is dependent on Asp, allowing nitrogen and source/sink status to act as a lever to control GH3.5 function in growth hormone vs. defense hormone homeostasis. By integrating information on GH3.5 enzyme kinetics, described herein, with knowledge of IAA, SA, and Asp concentrations *in planta* and *GH3.5* expression patterns, we developed a model that illustrates the dual function of GH3.5 *in planta* to regulate auxin homeostasis during growth or salicylic acid homeostasis during defense (Fig. 5).

While there are no other reported *Arabidopsis* GH3 enzymes that are active on SA, we do not explicitly address potential contributions from other GH3 enzymes active on IAA. In particular, AtGH3.6 is highly similar to AtGH3.5 (Okrent and Wildermuth, 2011). Kinetic analyses have not been performed on AtGH3.6, but endpoint assays indicate it also prefers Asp as the amino acid substrate (Staswick et al., 2005). Furthermore, overexpression of *AtGH3.5* or *AtGH3.6* can result in enhanced accumulation of IAA-Asp (Park et al., 2007a; Staswick et al., 2005; Westfall et al., 2016). There is some overlap in *AtGH3.5* and *AtGH3.6* expression patterns (Winter et al., 2007) suggesting functional redundancy and/or fine-tuning via paralogous genes; however only *AtGH3.5* is induced in response to SA (Goda et al., 2008) and the obligate biotrophic powdery mildew *G. orontii* concordant with SA accumulation (Chandran et al., 2009).

### 3.1. Plant nitrogen flux through Asp contributes to GH3.5 specificity

Asp is a central metabolic amino acid required for synthesis of Lys, Thr, Met, and Ile, and induced plant defense systemic signals such as the Lys degradation product pipecolic acid. (Galili, 2011; Less et al., 2010; Li et al., 2014; Návarová et al., 2012; Stuttmann et al., 2011; Vidal et al., 2014). Along with Glu, Gln, and Asn, Asp controls nitrogen flux through the plant and is associated with local nitrogen transport in source tissue (Gaufichon et al., 2013, 2010; Lea et al., 2007). Physiologically relevant values of Asp in plants range from 0.12 mM to 3 mM based on analytical quantification and $K_m$ values for plant enzymes that use Asp as a substrate (e.g. Besnard et al., 2016; Buhtz et al., 2015; Curien et al., 2007; Lin and Wu, 2004; Miesak and Coruzzi, 2002; Návarová et al., 2012; Torre et al., 2006; Watanabe et al., 2013).

Nitrogen mobilization is important not only during development, but also in plant-pathogen interactions as it affects pathogen access to nutrients and plant defense resource allocation (Gupta et al., 2013; Snoeijers et al., 2000). Mature leaves exhibit relatively low Asp levels that can be further reduced in response to pathogen (e.g. Návarová et al., 2012). Therefore, the dependence of GH3.5 catalytic efficiency for IAA vs. SA on Asp can act to integrate nitrogen and source/sink status with GH3.5 function in growth vs. defense hormone homeostasis.

### 3.2. Function of GH3.5 in auxin homeostasis at local auxin maxima

GH3.5 kinetics show a $K_m$ of ~20 µM for IAA independent of Asp concentration (Table 2). This IAA concentration is high and is associated with local IAA cellular maxima, for example with organ initiation and polar growth (Aloni et al., 2003; Bohn-Courseau, 2010; Marchant et al., 2002; Sabatini et al., 1999; Tanaka et al., 2006). Similarly, *GH3.5* is specifically expressed in these cells (Brady et al., 2007; Winter et al., 2007; Zhang et al., 2008). Approximate cellular concentrations for auxin are based on studies using the *DR5* promoter driving *GUS* gene expression (*DR5::GUS*), which has a functional range of 100 nM to 100 µM IAA (Sabatini et al., 1999; Ulmasov et al., 1997), the DII-VENUS sensor (1 nM–1 µM IAA functional range; Brunoud et al., 2012) and GC-MS analysis of extracted plant tissue (e.g., Tam et al., 2000; Uggla et al., 1996). For example, *DR5::GUS* accumulates at the lateral root primordium

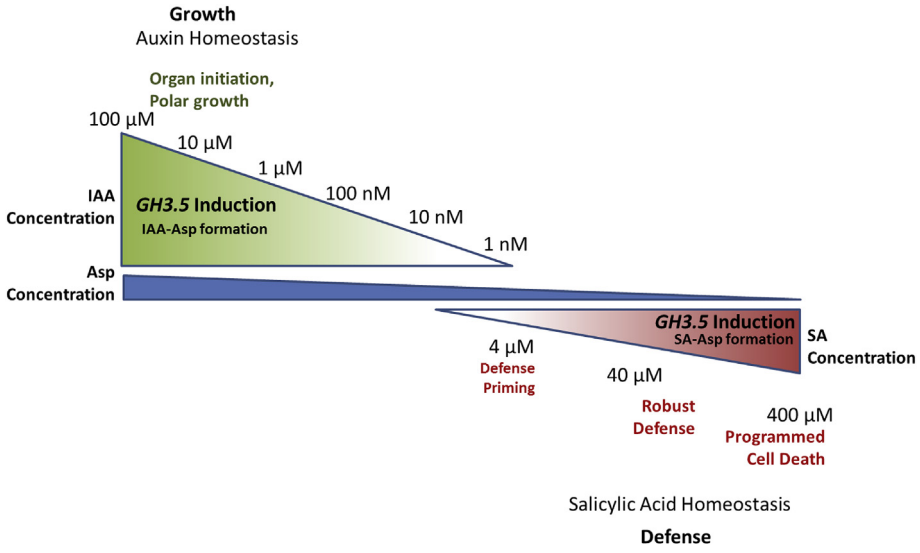


**Fig. 5. Model for GH3.5 function as a mediator of growth vs defense**. Localized high levels of auxin are associated with meristematic cells, organ initiation, and polar growth, and *GH3.5* is specifically expressed in these cells. For leaves, younger developing leaves exhibit moderate levels of IAA and high Asp. As leaves mature and senesce and/or are infected by a pathogen, the concentrations of IAA and Asp decrease. By contrast, SA increases with senescence and is induced dramatically by (hemi)-biotrophic pathogens. *GH3.5* is also induced by these pathogens concordant with SA accumulation. The kinetics of GH3.5 dependence on Asp show a dramatic preference for IAA when Asp is high, consistent with GH3.5 function to regulate IAA homeostasis via conversion of IAA to inactive IAA-Asp during growth/development when both IAA and Asp are high. Decreasing Asp through age and/or stress creates more favorable conditions for GH3.5 conjugation of SA to SA-Asp, thereby controlling SA homeostasis and defense. See text for additional details.

(Mei et al., 2012) where *GH3.5* is expressed (Brady et al., 2007; Winter et al., 2007; Zhang et al., 2008). Concordantly, there is a 7-fold increase in IAA-Asp in 10 day old roots of plants in which *GH3.5* is overexpressed (*wes1-D*) and fewer lateral roots are formed, whereas there is a 2-fold decrease in IAA-Asp levels in *gh3.5/wes1* knockout lines compared to wild type (Park et al., 2007a). Taken together, these data strongly support a functional role for GH3.5 as a means of spatially and temporally limiting active auxin during organ initiation/polar growth through its irreversible conversion to the inactive IAA-Asp, which is designated for catabolism (Ostin et al., 1998; Woodward and Bartel, 2005).

Consistent with our kinetic data for GH3.5 and model (Fig. 5), modeling of auxin homeostasis indicates that GH3-mediated degradation of auxin (e.g. to IAA-Asp) is critical to IAA homeostasis when [auxin] is high, whereas degradation via oxidation operates at low auxin levels (Mellor et al., 2016). The high rate of auxin conjugation to form IAA-Asp has long been noted in response to exogenously supplied auxin (e.g., Andreae and Good, 1955). And, a detailed examination of auxin metabolism rates as reported in Kramer and Ackelsberg (2015) supports our kinetic studies and functional model (Fig. 5), suggesting that GH3.5 conjugation of IAA to IAA-Asp spatially controls local IAA maxima. As SA levels in developing tissue are very low (discussed further below), GH3.5 would not be active on SA. Moreover, given high [Asp] in developing tissue, the catalytic efficiency of GH3.5 would be 357-fold higher with IAA vs. SA (Table 2).

### 3.3. Function of GH3.5 in induced SA homeostasis

Our kinetic analyses indicate a role for GH3.5 in SA homeostasis under conditions when SA is elevated and auxin and Asp concentrations are low, such as during infection of mature leaves by (hemi)-biotrophic pathogens. Unless specifically produced/manipulated by the pathogen, [IAA] is very low in mature fully expanded leaves (Marchant et al., 2002; Staswick et al., 2005). By contrast, SA levels in leaves rise dramatically with infection by (hemi)-biotrophs (Dempsey et al., 2011).

Approximate cellular concentrations for SA have been deduced from analytical measurements of SA extracted from plant tissue (e.g., Meuwly and Metraux, 1993; Müller et al., 2002), utilization of an SA responsive *Acetinobacter* reporter strain in tobacco (0.1–400 µM SA functional range; Huang et al., 2006), expression *of PR-1::GUS* as a proxy for robust SA accumulation associated with local defense (Dempsey et al., 2011), and knowledge of the $K_m$s for enzymes that utilize SA as their *in planta* substrate. In tobacco, spatially resolved SA analysis in response to tobacco mosaic virus or a fungal HR elicitor showed zones of concentration-dependent SA accumulation and associated defense response (Dorey et al., 1997; Huang et al., 2006). SA concentrations increased from below detection (0.1 µM) to 380 µM in localized spots preceding HR cell death (Huang et al., 2006). Cells in areas neighboring the HR site exhibited free SA of ~75–200 µM, consistent with robust local defense, while distal cells exhibited minimal SA (e.g. 10 µM) associated with defense priming or no appreciable SA. Furthermore, knowledge of the $K_m$s for SA of enzymes involved in SA priming (SA methyltranferase, $K_m = 16$ µM; Chen et al., 2003) or conjugating SA to reversible SA-glucosides as part of robust local defense (SA glucosyltransferases: $K_m$'s ~200 µM; Lim et al., 2002; Song, 2006) support the approximate [SA] ranges and associated functional activities shown in Fig. 5. Therefore, in response to (hemi)biotrophic pathogens, cellular SA concentrations are in the range of 4–400 µM depending on the specific pathogen-host interaction, the time frame, and specific cell.

Concordant with SA accumulation, *GH3.5* expression is induced in *Arabidopsis* leaves in response to (hemi)-biotrophic pathogens including *Pseudomonas syringae*, *Hyaloperonospora arabidopsidis*, and *Golvovinomyces orontii* (Chandran et al., 2009; Wang et al., 2011; Winter et al., 2007; Zhang et al., 2007). Use of a *GH3.5::GUS* reporter showed strongest *GH3.5* expression in response to *P. syringae* pathogens at the edge of the pathogen infiltration zone with some extension into the surrounding vasculature and cells (Zhang et al., 2008).

What then could be the function of GH3.5 in SA homeostasis in response to these pathogens? Our kinetic data for GH3.5 suggests

that it could operate to mediate SA homeostasis in SA functional ranges involved in defense priming or local robust defense (Fig. 5). SA-Asp is not hydrolyzed back to active SA nor is it able to induce robust *PR-1* expression associated with local defense (Chen et al., 2013). Therefore, conversion of SA to SA-Asp could irreversibly inactivate SA in specific cells, confining robust defense. It could even act to limit the extent of HR and PCD by converting accumulating free SA to SA-Asp, thereby preventing SA levels from rising to a threshold associated with PCD. Alternatively, as SA-Asp was able to induce very low level *PR-1* expression at levels associated with defense priming (Chen et al., 2013) and there is a possibility that it is mobile (Chen et al., 2013), it could potentially act to promote defense priming within a leaf or systemically.

### 3.4. Concluding summary for GH3.5 role in modulating growth vs. defense outcomes

Herein, we show how GH3.5, with dual activity on IAA and SA, can integrate cellular metabolic status via Asp to provide fine control of growth vs. defense outcomes and hormone homeostasis (Fig. 5). During active growth, [IAA] and [Asp] are high and the catalytic efficiency ($k_{cat}/K_m$) of GH3.5 for IAA is 360-fold higher than with SA. *GH3.5* is expressed under these conditions and conversion of IAA to inactive IAA-Asp would provide fine spatial and temporal control over local auxin developmental responses such as lateral root initiation. By contrast, [SA] is dramatically elevated in response to (hemi)-biotrophic pathogens. Under these conditions, [Asp] is low and GH3.5 has equal affinity ($K_m$) for SA and IAA with similar catalytic efficiencies. The concentration of IAA tends to be very low under these conditions, well below the $K_m$ for IAA. *GH3.5* is induced by these pathogens and the elevated [SA] would favor GH3.5 catalyzed formation of SA-Asp, fine-tuning localized defensive responses.

## 4. Experimental

### 4.1. AtGH3.5 expression and purification

*AtGH3.5* cDNA was amplified and inserted into a pET-28a vector (Novagen), then expressed in *Escherichia coli* Rosetta2 (DE3) cells, as in (Okrent et al., 2009). Purification of His-GH3.5 was done with nickel-nitriolotriacetic acid His-Bind resin (Novagen) according to manufacturer's directions and run on an SDS-PAGE gel. No other proteins were present. Initially, the His tag was cleaved with Thrombin (Novagen), but kinetic assays testing GH3.5 vs His-GH3.5 showed no difference in enzyme activity, so His-GH3.5 was used for experiments. Protein concentration was quantified using a Bradford assay with a 96-well plate using Coomassie Blue G-250 (EM Biosciences). Bovine serum albumin was used as a standard. Protein was dialyzed into 100 mM Tris, pH 7.7, 10% glycerol, and 1 mM DTT and stored at −80 °C. Assays were repeated with enzyme from different batches to confirm results.

### 4.2. Determination of kinetic parameters: adenylation

His-GH3.5 activity was measured spectrophotometrically at 340 nm using pyrophosphate reagent (Sigma). The production of pyrophosphate after adenylation is coupled to fructose-6-phophate kinase, adolase, triose-phosphate isomerase, and glycerophosphate dehydrogenase ending with the oxidation of NADH to $NAD^+$, visible by absorbance at 340 nm and measured with a Spectromax Plus microplate spectrophotometer (Molecular Devices) at 340 nm using SOFTMax PRO 3.0 (Molecular Devices) software. 1 mM DTT, 5 mM MgCl2, 2.5 mM ATP and 10–20 μg of His-GH3.5 were added. Pyrophosphate reagent (Sigma) vials were reconstituted in 4 mL double distilled $H_2O$ and 65 μl was used in each 200 μl reaction.

### 4.3. Determination of kinetic parameters: full reaction

His-GH3.5 activity was measured using a coupled, high-throughput spectrophotometric assay. Briefly, the reaction coupled the release of AMP to the conversion of NADH to $NAD^+$ using myokinase, pyruvate kinase, and lactate dehydrogenase, as described in (Chen et al., 2010). Loss of NADH was measured with a Spectromax Plus microplate spectrophotometer (Molecular Devices) at 340 nm using SOFTMax PRO 3.0 (Molecular Devices) software. Assays were conducted in 200 μl volumes in 96 well plates in 20 mM Tris (pH 8.0), 5 mM $MgCl_2$, 20 mM ATP, 20 mM phosphoenolpyruvate, 2 mM NADH and 1 mM DTT with 20 μg GH3.5 and 4 units each of myokinase, pyruvate kinase, and lactate dehydrogenase.

### 4.4. Kinetic data analysis

Substrates were added immediately prior to loading into Spectromax Plus microplate spectrophotometer (Molecular Devices) for absorbance measurements at 340 nm every 15–20 s for 20–60 min. All experiments were repeated 2 to 5 times with similar results. The velocity of a no GH3.5 control was subtracted and for comparison between assays, velocities were normalized to zero. The extinction coefficient for NADH, 6.22 $\mu M^{-1} * cm^{-1}$ was used for conversion of velocities from Δabsorbance/min to μmol/min. Estimates of kinetic parameters were initially determined using the Hanes-Woolf equation fit to initial velocity values, then refined with Kaleidagraph (Synergy Software).

## Acknowledgements

We thank Michael Steinwand for assistance with protein modeling and critical review of the manuscript. This work was supported by a National Science Foundation (NSF) Graduate Research Fellowship to R.M., the UC Berkeley William Carrol Smith Graduate Research Fellowship in Plant Pathology to R.A.O., and NSF IOS-1449110 to M.C.W.

## References

Adamowski, M., Friml, J., 2015. PIN-dependent auxin transport: action, regulation, and evolution. Plant Cell Online 27, 20–32. http://dx.doi.org/10.1105/tpc.114.134874.

Aloni, R., Schwalm, K., Langhans, M., Ullrich, C.I., 2003. Gradual shifts in sites of free-auxin production during leaf-primordium development and their role in vascular differentiation and leaf morphogenesis in Arabidopsis. Planta 216, 841–853. http://dx.doi.org/10.1007/S00425-002-0937-8.

Andreae, W.A., Good, N.E., 1955. The formation of indoleacetylaspartic acid in pea seedlings. Plant Physiol. 30, 380–382.

Besnard, J., Pratelli, R., Zhao, C., Sonawala, U., Collakova, E., Pilot, G., Okumoto, S., 2016. UMAMIT14 is an amino acid exporter involved in phloem unloading in Arabidopsis roots. J. Exp. Bot. 67, 6385–6397. http://dx.doi.org/10.1093/jxb/erw412.

Bohn-Courseau, I., 2010. Auxin: a major regulator of organogenesis. C. R. Biol. 333, 290–296. http://dx.doi.org/10.1016/j.crvi.2010.01.004.

Böttcher, C., Dennis, E.G., Booker, G.W., Polyak, S.W., Boss, P.K., Davies, C., 2012. A novel tool for studying auxin-metabolism: the inhibition of grapevine indole-3-acetic acid-amido synthetases by a reaction intermediate analogue. PLoS One 7, e37632. http://dx.doi.org/10.1371/journal.pone.0037632.

Bourne, D.J., Barrow, K.D., Milborrow, B.V., 1991. Salicyloylaspartate as an endogenous component in the leaves of Phaseolus vulgaris. Phytochemistry 30, 4041–4044.

Brady, S.M., Orlando, D.A., Lee, J.-Y., Wang, J.Y., Koch, J., Dinneny, J.R., Mace, D., Ohler, U., Benfey, P.N., 2007. A high-resolution root spatiotemporal map reveals dominant expression patterns. Science (80-. ) 318, 801–806. http://dx.doi.org/10.1126/science.1146265.

Brunoud, G., Wells, D.M., Oliva, M., Larrieu, A., Mirabet, V., Burrow, A.H., Beeckman, T., Kepinski, S., Traas, J., Bennett, M.J., Vernoux, T., 2012. A novel sensor to map auxin response and distribution at high spatio-temporal resolution. Nature 482, 103–106. http://dx.doi.org/10.1038/nature10791.

Buhtz, A., Witzel, K., Strehmel, N., Ziegler, J., Abel, S., Grosch, R., 2015. Perturbations in the primary metabolism of tomato and *Arabidopsis thaliana* plants infected with the soil-borne fungus Verticillium dahliae. PLoS One 10, e0138242. http://dx.doi.org/10.1371/journal.pone.0138242.

Canet, J.V., Dobón, A., Ibáñez, F., Perales, L., Tornero, P., 2010. Resistance and biomass in Arabidopsis: a new model for salicylic acid perception. Plant Biotechnol. J. 8, 126–141. http://dx.doi.org/10.1111/j.1467-7652.2009.00468.x.

Chandran, D., Rickert, J., Huang, Y., Steinwand, M.A., Marr, S.K., Wildermuth, M.C., 2014. Atypical E2F transcriptional repressor DEL1 acts at the intersection of plant growth and immunity by controlling the hormone salicylic acid. Cell Host Microbe 15, 506–513. http://dx.doi.org/10.1016/j.chom.2014.03.007.

Chandran, D., Tai, Y.C., Hather, G., Dewdney, J., Denoux, C., Burgess, D.G., Ausubel, F.M., Speed, T.P., Wildermuth, M.C., 2009. Temporal global expression data reveal known and novel salicylate-impacted processes and regulators mediating powdery mildew growth and reproduction on Arabidopsis. Plant Physiol. 149, 1435–1451. http://dx.doi.org/10.1104/pp.108.132985.

Chen, F., D'Auria, J.C., Tholl, D., Ross, J.R., Gershenzon, J., Noel, J.P., Pichersky, E., 2003. An *Arabidopsis thaliana* gene for methylsalicylate biosynthesis, identified by a biochemical genomics approach, has a role in defense. Plant J. 36, 577–588.

Chen, Q., Westfall, C.S., Hicks, L.M., Wang, S., Jez, J.M., 2010. Kinetic basis for the conjugation of auxin by a GH3 family indole-acetic acid-amido synthetase. J. Biol. Chem. 285, 29780–29786. http://dx.doi.org/10.1074/jbc.M110.146431.

Chen, Q., Zhang, B., Hicks, L.M., Wang, S., Jez, J.M., 2009. A liquid chromatography-tandem mass spectrometry-based assay for indole-3-acetic acid-amido synthetase. Anal. Biochem. 390, 149–154. http://dx.doi.org/10.1016/j.ab.2009.04.027.

Chen, Y., Shen, H., Wang, M., Li, Q., He, Z., 2013. Salicyloyl-aspartate synthesized by the acetyl-amido synthetase GH3. 5 is a potential activator of plant immunity in Arabidopsis. Acta Biochim. Biophys. Sin. 45, 827–836. http://dx.doi.org/10.1093/abbs/gmt078.Advance.

Curien, G., Laurencin, M., Robert-Genthon, M., Dumas, R., 2007. Allosteric monofunctional aspartate kinases from *Arabidopsis*. FEBS J. 274, 164–176. http://dx.doi.org/10.1111/j.1742-4658.2006.05573.x.

Dempsey, D.A., Vlot, A.C., Wildermuth, M.C., Klessig, D.F., 2011. Salicylic Acid biosynthesis and metabolism. Arab. Book 9, e0156. http://dx.doi.org/10.1199/tab.0156.

Denancé, N., Sánchez-Vallet, A., Goffner, D., Molina, A., 2013. Disease resistance or growth: the role of plant hormones in balancing immune responses and fitness costs. Front. Plant Sci. 4, 155. http://dx.doi.org/10.3389/fpls.2013.00155.

Dewdney, J., Reuber, T.L., Wildermuth, M.C., Devoto, A., Cui, J., Stutius, L.M., Drummond, E.P., Ausubel, F.M., 2000. Three unique mutants of Arabidopsis identify eds loci required for limiting growth of a biotrophic fungal pathogen. Plant J. 24, 205–218. http://dx.doi.org/10.1046/j.1365-313x.2000.00870.x.

Dorey, S., Baillieul, F., Pierrel, M.-A., Saindrenan, P., Fritig, B., Kauffmann, S., 1997. Spatial and temporal induction of cell death, defense genes, and accumulation of salicylic acid in tobacco leaves reacting hypersensitively to a fungal glycoprotein elicitor. Mol. Plant-Microbe Interact. 10, 646–655. http://dx.doi.org/10.1094/MPMI.1997.10.5.646.

Fu, Z.Q., Yan, S., Saleh, A., Wang, W., Ruble, J., Oka, N., Mohan, R., Spoel, S.H., Tada, Y., Zheng, N., Dong, X., 2012. NPR3 and NPR4 are receptors for the immune signal salicylic acid in plants. Nature 486, 228–232. http://dx.doi.org/10.1038/nature11162.

Galili, G., 2011. The aspartate-family pathway of plants: linking production of essential amino acids with energy and stress regulation. Plant Signal. Behav. 6, 192–195.

Gaufichon, L., Masclaux-Daubresse, C., Tcherkez, G., Reisdorf-Cren, M., Sakakibara, Y., Hase, T., Clément, G., Avice, J.-C., Grandjean, O., Marmagne, A., Boutet-Mercey, S., Azzopardi, M., Soulay, F., Suzuki, A., 2013. *Arabidopsis thaliana* ASN2 encoding asparagine synthetase is involved in the control of nitrogen assimilation and export during vegetative growth. Plant. Cell Environ. 36, 328–342. http://dx.doi.org/10.1111/j.1365-3040.2012.02576.x.

Gaufichon, L., Reisdorf-Cren, M., Rothstein, S.J., Chardon, F., Suzuki, A., 2010. Biological functions of asparagine synthetase in plants. Plant Sci. 179, 141–153. http://dx.doi.org/10.1016/j.plantsci.2010.04.010.

Geu-Flores, F., Møldrup, M.E., Böttcher, C., Olsen, C.E., Scheel, D., Halkier, B.A., 2011. Cytosolic γ-glutamyl peptidases process glutathione conjugates in the biosynthesis of glucosinolates and camalexin in Arabidopsis. Plant Cell 23, 2456–2469. http://dx.doi.org/10.1105/tpc.111.083998.

Goda, H., Sasaki, E., Akiyama, K., Maruyama-Nakashita, A., Nakabayashi, K., Li, W., Ogawa, M., Yamauchi, Y., Preston, J., Aoki, K., Kiba, T., Takatsuto, S., Fujioka, S., Asami, T., Nakano, T., Kato, H., Mizuno, T., Sakakibara, H., Yamaguchi, S., Nambara, E., Kamiya, Y., Takahashi, H., Hirai, M.Y., Sakurai, T., Shinozaki, K., Saito, K., Yoshida, S., Shimada, Y., 2008. The AtGenExpress hormone- and chemical-treatment data set: experimental design, data evaluation, model data analysis, and data access. Plant J. 0 http://dx.doi.org/10.1111/j.0960-7412.2008.03510.x, 80414150319983.

Gupta, K.J., Brotman, Y., Segu, S., Zeier, T., Zeier, J., Persijn, S.T., Cristescu, S.M., Harren, F.J.M., Bauwe, H., Fernie, A.R., Kaiser, W.M., Mur, L.A.J., 2013. The form of nitrogen nutrition affects resistance against Pseudomonas syringae pv. phaseolicola in tobacco. J. Exp. Bot. 64, 553–568. http://dx.doi.org/10.1093/jxb/ers348.

Hagemeier, J., Schneider, B., Oldham, N.J., Hahlbrock, K., 2001. Accumulation of soluble and wall-bound indolic metabolites in *Arabidopsis thaliana* leaves infected with virulent or avirulent Pseudomonas syringae pathovar tomato strains. Proc. Natl. Acad. Sci. 98, 753–758. http://dx.doi.org/10.1073/pnas.98.2.753.

Huang, W.E., Huang, L., Preston, G.M., Naylor, M., Carr, J.P., Li, Y., Singer, A.C., Whiteley, A.S., Wang, H., 2006. Quantitative *in situ* assay of salicylic acid in tobacco leaves using a genetically modified biosensor strain of *Acinetobacter* sp. ADP1. Plant J. 46, 1073–1083. http://dx.doi.org/10.1111/j.1365-313X.2006.02758.x.

Jaillais, Y., Chory, J., 2010. Unraveling the paradoxes of plant hormone signaling integration. Nat. Struct. Mol. Biol. 17, 642–645. http://dx.doi.org/10.1038/nsmb0610-642.

Kepinski, S., Leyser, O., 2005. The Arabidopsis F-box protein TIR1 is an auxin receptor. Nature 435, 446–451.

Klein, A.P., Anarat-Cappillino, G., Sattely, E.S., 2013. Minimum set of cytochromes P450 for reconstituting the biosynthesis of camalexin, a major Arabidopsis antibiotic. Angew. Chem. Int. Ed. Engl. 52, 13625–13628. http://dx.doi.org/10.1002/anie.201307454.

Kramer, E.M., Ackelsberg, E.M., 2015. Auxin metabolism rates and implications for plant development. Front. Plant Sci. 6, 150. http://dx.doi.org/10.3389/fpls.2015.00150.

Lea, P.J., Sodek, L., Parry, M.A.J., Shewry, P.R., Halford, N.G., 2007. Asparagine in plants. Ann. Appl. Biol. 150, 1–26. http://dx.doi.org/10.1111/j.1744-7348.2006.00104.x.

Less, H., Angelovici, R., Tzin, V., Galili, G., 2010. Principal transcriptional regulation and genome-wide system interactions of the Asp-family and aromatic amino acid networks of amino acid metabolism in plants. Amino Acids 39, 1023–1028. http://dx.doi.org/10.1007/s00726-010-0566-7.

Li, Y., Krouk, G., Coruzzi, G.M., Ruffel, S., 2014. Finding a nitrogen niche: a systems integration of local and systemic nitrogen signalling in plants. J. Exp. Bot. 65, 5601–5610. http://dx.doi.org/10.1093/jxb/eru263.

Lim, E.-K., Doucet, C.J., Li, Y., Elias, L., Worrall, D., Spencer, S.P., Ross, J., Bowles, D.J., 2002. The activity of ArabidopsisGlycosyltransferases toward salicylic acid, 4-hydroxybenzoic acid, and other benzoates. J. Biol. Chem. 277, 586–592. http://dx.doi.org/10.1074/jbc.M109287200.

Lin, J.-F., Wu, S.-H., 2004. Molecular events in senescing *Arabidopsis* leaves. Plant J. 39, 612–628. http://dx.doi.org/10.1111/j.1365-313X.2004.02160.x.

Malamy, J., Car, J.P., Klessig, D.F., Raskin, I., 1990. Salicylic acid: a likely endogenous signal in the resistance response of tobacco to viral infection. Science (80-. ) 250, 1002–1004.

Marchant, A., Bhalerao, R., Casimiro, I., Eklöf, J., Casero, P.J., Bennett, M., Sandberg, G., 2002. AUX1 promotes lateral root formation by facilitating indole-3-acetic acid distribution between sink and source tissues in the Arabidopsis seedling. Plant Cell 14, 589–597. http://dx.doi.org/10.1105/TPC.010354.

Mei, Y., Jia, W.-J., Chu, Y.-J., Xue, H.-W., 2012. Arabidopsis phosphatidylinositol monophosphate 5-kinase 2 is involved in root gravitropism through regulation of polar auxin transport by affecting the cycling of PIN proteins. Cell Res. 22, 581–597. http://dx.doi.org/10.1038/cr.2011.150.

Mellor, N., Band, L.R., Pěnčík, A., Novák, O., Rashed, A., Holman, T., Wilson, M.H., Voß, U., Bishopp, A., King, J.R., Ljung, K., Bennett, M.J., Owen, M.R., 2016. Dynamic regulation of auxin oxidase and conjugating enzymes *AtDAO1* and *GH3* modulates auxin homeostasis. Proc. Natl. Acad. Sci. 113, 11022–11027. http://dx.doi.org/10.1073/pnas.1604458113.

Meuwly, P., Metraux, J.P., 1993. Ortho-anisic acid as internal standard for the simultaneous quantitation of salicylic acid and its putative biosynthetic precursors in cucumber leaves. Anal. Biochem. 214, 500–505. http://dx.doi.org/10.1006/abio.1993.1529.

Miesak, B.H., Coruzzi, G.M., 2002. Molecular and physiological analysis of Arabidopsis mutants defective in cytosolic or chloroplastic aspartate aminotransferase. Plant Physiol. 129, 650–660. http://dx.doi.org/10.1104/pp.005090.

Møldrup, M.E., Geu-Flores, F., Halkier, B.A., 2013. Assigning gene function in biosynthetic pathways: camalexin and beyond. Plant Cell 25, 360–367. http://dx.doi.org/10.1105/tpc.112.104745.

Müller, A., Düchting, P., Weiler, E., 2002. A multiplex GC-MS/MS technique for the sensitive and quantitative single-run analysis of acidic phytohormones and related compounds, and its application to *Arabidopsis thaliana*. Planta 216, 44–56. http://dx.doi.org/10.1007/s00425-002-0866-6.

Návarová, H., Bernsdorff, F., Döring, A.-C., Zeier, J., 2012. Pipecolic acid, an endogenous mediator of defense amplification and priming, is a critical regulator of inducible plant immunity. Plant Cell 24, 5123–5141. http://dx.doi.org/10.1105/tpc.112.103564.

Okrent, R.A., Brooks, M.D., Wildermuth, M.C., 2009. Arabidopsis GH3.12 (PBS3) conjugates amino acids to 4-substituted benzoates and is inhibited by salicylate. J. Biol. Chem. 284, 9742–9754. http://dx.doi.org/10.1074/jbc.M806662200.

Okrent, R.A., Wildermuth, M.C., 2011. Evolutionary history of the GH3 family of acyl adenylases in rosids. Plant Mol. Biol. 76, 489–505. http://dx.doi.org/10.1007/s11103-011-9776-y.

Ostin, a, Kowalyczk, M., Bhalerao, R.P., Sandberg, G., 1998. Metabolism of indole-3-acetic acid in Arabidopsis. Plant Physiol. 118, 285–296.

Park, J.-E., Park, J.-Y., Kim, Y.-S., Staswick, P.E., Jeon, J., Yun, J., Kim, S.-Y., Kim, J., Lee, Y.-H., Park, C.-M., 2007a. GH3-mediated auxin homeostasis links growth regulation with stress adaptation response in Arabidopsis. J. Biol. Chem. 282, 10036–10046. http://dx.doi.org/10.1074/jbc.M610524200.

Park, S.-W., Kaimoyo, E., Kumar, D., Mosher, S., Klessig, D.F., 2007b. Methyl salicylate is a critical mobile signal for plant systemic acquired resistance. Science 318, 113–116. http://dx.doi.org/10.1126/science.1147113.

Peat, T.S., Böttcher, C., Newman, J., Lucent, D., Cowieson, N., Davies, C., 2012. Crystal structure of an indole-3-acetic acid amido synthetase from grapevine involved in auxin homeostasis. Plant Cell 24, 4525–4538. http://dx.doi.org/10.1105/tpc.112.102921.

Pettersen, E.F., Goddard, T.D., Huang, C.C., Couch, G.S., Greenblatt, D.M., Meng, E.C.,

Ferrin, T.E., 2004. UCSF Chimera—a visualization system for exploratory research and analysis. J. Comput. Chem. 25, 1605–1612. http://dx.doi.org/10.1002/jcc.20084.
Rampey, R.A., Leclere, S., Kowalczyk, M., Ljung, K., Bartel, B., Biology, C., Texas, R.A.R., 2004. A family of auxin-conjugate hydrolases that contributes to free indole-3-acetic acid levels during Arabidopsis germination 1. Plant Physiol. 135, 978–988. http://dx.doi.org/10.1104/pp.104.039677.978.
Rasmussen, J.B., Hammerschmidt, R., Zook, M.N., 1991. Systemic induction of salicylic acid accumulation in cucumber after inoculation with Pseudomonas syringae pv syringae. Plant Physiol. 97, 1342–1347.
Robert-Seilaniantz, A., Grant, M., Jones, J.D.G., 2011a. Hormone crosstalk in plant disease and defense: more than just jasmonate-salicylate antagonism. Annu. Rev. Phytopathol. 49, 317–343. http://dx.doi.org/10.1146/annurev-phyto-073009-114447.
Robert-Seilaniantz, A., MacLean, D., Jikumaru, Y., Hill, L., Yamaguchi, S., Kamiya, Y., Jones, J.D.G., 2011b. The microRNA miR393 re-directs secondary metabolite biosynthesis away from camalexin and towards glucosinolates. Plant J. 67, 218–231. http://dx.doi.org/10.1111/j.1365-313X.2011.04591.x.
Sabatini, S., Beis, D., Wolkenfelt, H., Murfett, J., Guilfoyle, T., Malamy, J., Benfey, P., Leyser, O., Bechtold, N., Weisbeek, P., Scheres, B., 1999. An auxin-dependent distal organizer of pattern and polarity in the Arabidopsis root. Cell 99, 463–472. http://dx.doi.org/10.1016/S0092-8674(00)81535-4.
Schlicht, M., Ludwig-Müller, J., Burbach, C., Volkmann, D., Baluska, F., 2013. Indole-3-butyric acid induces lateral root formation via peroxisome-derived indole-3-acetic acid and nitric oxide. New Phytol. 200, 473–482. http://dx.doi.org/10.1111/nph.12377.
Snoeijers, S.S., Pérez-García, A., Joosten, M.H.A.J., De Wit, P.J.G.M., 2000. The effect of nitrogen on disease development and gene expression in bacterial and fungal plant pathogens. Eur. J. Plant Pathol. 106, 493–506. http://dx.doi.org/10.1023/A:1008720704105.
Song, J.T., 2006. Induction of a salicylic acid glucosyltransferase, AtSGT1, is an early disease response in *Arabidopsis thaliana*. Mol. Cells 22, 233–238.
Spoel, S.H., Dong, X., 2012. How do plants achieve immunity? Defence without specialized immune cells. Nat. Rev. Immunol. 12, 89–100. http://dx.doi.org/10.1038/nri3141.
Staswick, P.E., Serban, B., Rowe, M., Tiryaki, I., 2005. Characterization of an Arabidopsis enzyme family that conjugates amino acids to indole-3-acetic acid. Plant Cell 17, 616–627. http://dx.doi.org/10.1105/tpc.104.026690.1.
Staswick, P.E., Tiryaki, I., Rowe, M.L., 2002. Jasmonate response locus JAR1 and several related Arabidopsis genes encode enzymes of the firefly luciferase superfamily that show activity on jasmonic, salicylic, and indole-3-acetic acids in an assay for adenylation. Plant Cell 14, 1405–1415. http://dx.doi.org/10.1105/tpc.000885.defect.
Steffan, H., Ziegler, A., Rapp, A., 1988. N-salicyloyl-aspartic acid: a new phenolic compound in grapevines. Vitis 27, 79–86.
Stuttmann, J., Hubberten, H.-M., Rietz, S., Kaur, J., Muskett, P., Guerois, R., Bednarek, P., Hoefgen, R., Parker, J.E., 2011. Perturbation of Arabidopsis amino acid metabolism causes incompatibility with the adapted biotrophic pathogen Hyaloperonospora arabidopsidis. Plant Cell 23, 2788–2803. http://dx.doi.org/10.1105/tpc.111.087684.
Su, T., Li, Y., Yang, H., Ren, D., 2013. Reply: complexity in camalexin biosynthesis. Plant Cell 25, 367–370. http://dx.doi.org/10.1105/tpc.113.109975.
Su, T., Xu, J., Li, Y., Lei, L., Zhao, L., Yang, H., Feng, J., Liu, G., Ren, D., 2011. Glutathione-indole-3-acetonitrile is required for camalexin biosynthesis in *Arabidopsis thaliana*. Plant Cell 23, 364–380. http://dx.doi.org/10.1105/tpc.110.079145.
Sugawara, S., Mashiguchi, K., Tanaka, K., Hishiyama, S., Sakai, T., Hanada, K., Kinoshita-Tsujimura, K., Yu, H., Dai, X., Takebayashi, Y., Takeda-Kamiya, N., Kakimoto, T., Kawaide, H., Natsume, M., Estelle, M., Zhao, Y., Hayashi, K.-I., Kamiya, Y., Kasahara, H., 2015. Distinct characteristics of indole-3-acetic acid and phenylacetic acid, two common auxins in plants. Plant Cell Physiol. 56, 1641–1654. http://dx.doi.org/10.1093/pcp/pcv088.
Tam, Y.Y., Epstein, E., Normanly, J., 2000. Characterization of auxin conjugates in Arabidopsis. Low steady-state levels of indole-3-acetyl-aspartate, indole-3-acetyl-glutamate, and indole-3-acetyl-glucose. Plant Physiol. 123, 589–596.
Tanaka, H., Dhonukshe, P., Brewer, P.B., Friml, J., 2006. Spatiotemporal asymmetric auxin distribution: a means to coordinate plant development. Cell. Mol. Life Sci. 63, 2738–2754. http://dx.doi.org/10.1007/s00018-006-6116-5.
Tao, Y., Ferrer, J.-L., Ljung, K., Pojer, F., Hong, F., Long, J.A., Li, L., Moreno, J.E., Bowman, M.E., Ivans, L.J., Cheng, Y., Lim, J., Zhao, Y., Ballaré, C.L., Sandberg, G., Noel, J.P., Chory, J., 2008. Rapid synthesis of auxin via a new tryptophan-dependent pathway is required for shade avoidance in plants. Cell 133, 164–176. http://dx.doi.org/10.1016/j.cell.2008.01.049.
Torre, F., De Santis, L., Suárez, M.F., Crespillo, R., Cánovas, F.M., 2006. Identification and functional analysis of a prokaryotic-type aspartate aminotransferase: implications for plant amino acid metabolism. Plant J. 46, 414–425. http://dx.doi.org/10.1111/j.1365-313X.2006.02713.x.
Uggla, C., Moritz, T., Sandberg, G., Sundberg, B., 1996. Auxin as a positional signal in pattern formation in plants. Proc. Natl. Acad. Sci. U. S. A. 93, 9282–9286. http://dx.doi.org/10.1073/pnas.93.17.9282.
Ulmasov, T., Murfett, J., Hagen, G., Guilfoyle, T.J., 1997. Aux/IAA proteins repress expression of reporter genes containing natural and highly active synthetic auxin response elements. Plant Cell 9, 1963–1971. http://dx.doi.org/10.1105/tpc.9.11.1963.
Vanneste, S., Friml, J., 2009. Auxin: a trigger for change in plant development. Cell 136, 1005–1016. http://dx.doi.org/10.1016/j.cell.2009.03.001.
Vidal, E.A., Moyano, T.C., Canales, J., Gutierrez, R.A., 2014. Nitrogen control of developmental phase transitions in *Arabidopsis thaliana*. J. Exp. Bot. 65, 5611–5618. http://dx.doi.org/10.1093/jxb/eru326.
Vlieghe, K., Boudolf, V., Beemster, G.T.S., Maes, S., Magyar, Z., Atanassova, A., de Almeida Engler, J., De Groodt, R., Inzé, D., De Veylder, L., 2005. The DP-E2F-like gene DEL1 controls the endocycle in *Arabidopsis thaliana*. Curr. Biol. 15, 59–63. http://dx.doi.org/10.1016/j.cub.2004.12.038.
Wang, M., Liu, X., Chen, Y., Xu, X., Yu, B., Zhang, S., 2012. Involvement in Camalexin Biosynthesis through Conjugation of Indole-3-Carboxylic Acid and Cysteine and Upregulation of Camalexin Biosynthesis Genes, 54, 471–485. http://dx.doi.org/10.1111/j.1744-7909.2012.01131.x.
Wang, W., Barnaby, J.Y., Tada, Y., Li, H., Tör, M., Caldelari, D., Lee, D., Fu, X.-D., Dong, X., 2011. Timing of plant immune responses by a central circadian regulator. Nature 470, 110–114. http://dx.doi.org/10.1038/nature09766.
Watanabe, M., Balazadeh, S., Tohge, T., Erban, A., Giavalisco, P., Kopka, J., Mueller-Roeber, B., Fernie, A.R., Hoefgen, R., 2013. Comprehensive dissection of spatiotemporal metabolic shifts in primary, secondary, and lipid metabolism during developmental senescence in Arabidopsis. Plant Physiol. 162, 1290–1310. http://dx.doi.org/10.1104/pp.113.217380.
Westfall, C.S., Sherp, A.M., Zubieta, C., Alvarez, S., Schraft, E., Marcellin, R., Ramirez, L., Jez, J.M., 2016. *Arabidopsis thaliana* GH3.5 acyl acid amido synthetase mediates metabolic crosstalk in auxin and salicylic acid homeostasis. Proc. Natl. Acad. Sci. U. S. A. 113, 13917–13922. http://dx.doi.org/10.1073/pnas.1612635113.
Westfall, C.S., Zubieta, C., Herrmann, J., Kapp, U., Nanao, M.H., Jez, J.M., 2012. Structural basis for prereceptor modulation of plant hormones by GH3 proteins. Science 336, 1708–1711. http://dx.doi.org/10.1126/science.1221863.
Wildermuth, M.C., Dewdney, J., Wu, G., Ausubel, F.M., 2001. Isochorismate synthase is required to synthesize salicylic acid for plant defence. Nature 414, 562–565. http://dx.doi.org/10.1038/35107108.
Winter, D., Vinegar, B., Nahal, H., Ammar, R., Wilson, G.V., Provart, N.J., 2007. An "Electronic Fluorescent Pictograph" browser for exploring and analyzing large-scale biological data sets. PLoS One 2, e718. http://dx.doi.org/10.1371/journal.pone.0000718.
Woodward, A.W., Bartel, B., 2005. Auxin: regulation, action, and interaction. Ann. Bot. 95, 707–735. http://dx.doi.org/10.1093/aob/mci083.
Wu, Y., Zhang, D., Chu, J.Y., Boyle, P., Wang, Y., Brindle, I.D., De Luca, V., Després, C., 2012. The Arabidopsis NPR1 protein is a receptor for the plant defense hormone salicylic acid. Cell Rep. 1, 639–647. http://dx.doi.org/10.1016/j.celrep.2012.05.008.
Zhang, Z., Li, Q., Li, Z., Staswick, P.E., Wang, M., Zhu, Y., He, Z., 2007. Dual regulation role of GH3.5 in salicylic acid and auxin signaling during Arabidopsis-Pseudomonas syringae interaction. Plant Physiol. 145, 450–464. http://dx.doi.org/10.1104/pp.107.106021.
Zhang, Z., Wang, M., Li, Z., Li, Q., He, Z., 2008. Arabidopsis GH3.5 regulates salicylic acid-dependent and both NPR1-dependent and independent defense responses. Plant Signal. Behav. 3, 537–542.